Control allocation of an arbitrary fully actuated multirotor aerial vehicle equipped with one-DOF vectoring rotors

Flávia P. Nery[1], José A. Bezerra[1], Davi A. Santos[1]

[1]*Dept. of Mechatronics, Aeronautics Institute of Technology*
Praça Marechal Eduardo Gomes, 50, São José dos Campos, 12228-900, São Paulo, Brazil
flaviafpn@ita.br, agnelo@ita.br, davists@ita.br

Abstract. The present paper deals with the control allocation of fully actuated multirotor aerial vehicles (MAVs) equipped with an arbitrary number of radially vectoring rotors. To tackle the problem, we consider a control architecture in which the control allocator is cascaded with the control laws. Therefore, the latter provide the resultant force-torque commands for the former to distribute them among the available actuators, which include the spinning and the vectoring motors. We formulate the control allocator through an optimization problem in which the rotor thrust vectors represented in body-fixed frames are the design variables. In this way, the control allocation equation becomes linear since it does not explicitly include the commands for the vectoring angles, which can be immediately obtained afterwards from the computed optimal thrust vectors. In the optimization problem, the thrust vectors are constrained according to given bounds on their magnitude and vectoring angle. It is noteworthy that, considering a minimal thrust magnitude generally greater than zero, the thrust vectors span non-convex sets, thus making the original problem a non-convex optimization. However, instead of dealing with such non-convex sets, we have replaced them by convex ones, thus given rise to a convex program that approximates the original problem. The method is widely evaluated by computer simulations on a hexa-rotor with all the six rotors equipped with a one-degree-of-freedom vectoring mechanism.

Keywords: Flight control, control allocation, multirotor aerial vehicle, unmanned aerial vehicle, thrust-vectoring.

1 Introduction

The increasing utilization of multirotor aerial vehicles (MAVs) in diverse applications such as transportation, emergency response, and surveillance (Höhrová et al. [1], Shakhatreh et al. [2]) require advanced control strategies to harness their full potential. Among these MAVs, those equipped with one-degree-of-freedom (1-DOF) vectoring rotors represent a significant advancement due to their ability to combine compact design with the flexibility and redundancy required for precise maneuvers in constrained environments (Kumar et al. [3]). However, these vehicles typically present a complex control challenge and, despite the considerable research conducted on the field of MAV control (Saied et al. [4]), there remains room for improvement in this particular configuration.

Based on the work done by Bezerra and Santos [5, 6], Silva and Santos [7], Kirchengast et al. [8], Park et al. [9], which focus on fixed-rotor MAVs, the present paper aims to advance control strategies for MAVs by proposing an optimal control allocation method for 1-DOF thrust vectoring multicopters that prevents the violation of bounds for both rotors and vectoring actuators. In particular, by considering a non-zero minimal thrust bound to avoid the rotors to stop spinning during the flight, the rotor thrust vectors sweep non-convex sets. These sets are approximated by inscribed polytopes in order to recast the problem as a convex optimization.

The next sections of this paper are organized as follows. Section 2 presents the allocation problem, which is then detailed as an optimization problem and solved in Section 3. Section 4 provides numerical evaluations of the proposed strategy and analyzes its main properties. Finally, Section 5 presents some concluding remarks.

2 Problem definiton

This section introduces the notation used throughout the paper, followed by the definition of a mechanical model for the MAV. Finally, the control allocation problem is stated.

2.1 Notation

Denote scalar quantities, vectors, and matrices, respectively, by lowercase italic, lowercase boldface, and uppercase boldface letters, *e.g.*, $a \in \mathbb{R}$, $\mathbf{a} \in \mathbb{R}^n$, and $\mathbf{A} \in \mathbb{R}^{n\times m}$. A geometric (Euclidian) vector and a geometric point are denoted, respectively, as $\vec{a}$ and A, while a column vector has its components denoted by $\mathbf{a} = (a_1, a_2, ..., a_n)$.

Let $\mathcal{S}_a \triangleq \{\vec{x}_a, \vec{y}_a, \vec{z}_a\}$ be an arbitrary basis in the three-dimensional space, where $\vec{x}_a$, $\vec{y}_a$, and $\vec{z}_a$ are perpendicular unit Euclidian vectors. A vector $\vec{v}$ represented (projected) in this basis is denoted as $\mathbf{v}_a \in \mathbb{R}^3$. The unit vectors $\mathbf{e}_1 \triangleq (1,0,0)$, $\mathbf{e}_2 \triangleq (0,1,0)$, and $\mathbf{e}_3 \triangleq (0,0,1)$ represent the canonical basis for the $\mathbb{R}^3$. The cross product of two vectors $\vec{v}$ and $\vec{u}$, $\vec{w} \triangleq \vec{v} \times \vec{u}$, is represented in $\mathcal{S}_a$ by $\mathbf{w}_a = [\mathbf{v}_a\times]\mathbf{u}_a \in \mathbb{R}^3$, where $\mathbf{v}_a = (v_1, v_2, v_3)$ and

$$[\mathbf{v}_a\times] \triangleq \begin{bmatrix} 0 & -v_3 & v_2 \\ v_3 & 0 & -v_1 \\ -v_2 & v_1 & 0 \end{bmatrix} \in \mathbb{R}^{3\times 3}.$$

2.2 Mechanical model

For a MAV with n radially vectoring rotors, we can define: a coordinate system for the body $(B, \mathcal{S}_b)$, with B usually being coincident with the center of gravity (CG) and $\mathcal{S}_b \triangleq \{\vec{x}_b, \vec{y}_b, \vec{z}_b\}$; n body-fixed rotor-centered coordinate systems $(S_i, \mathcal{S}_{r_i})$, with $\mathcal{S}_{r_i} \triangleq \{\vec{x}_{r_i}, \vec{y}_{r_i}, \vec{z}_{r_i}\}$, where $i \in \mathcal{I}_n \triangleq \{1, 2, ..., n\}$, $\vec{x}_{r_i}$ points from S_i to B and $\vec{z}_{r_i}$ is aligned with the i-th rotor and points upwards, in the direction of the rotor blades, when the rotor vectoring angle $\varepsilon_i = 0$; n rotor-fixed coordinate systems $(S_i, \mathcal{S}_{s_i})$, where $\mathcal{S}_{s_i}$ is rotated w.r.t. $\mathcal{S}_{r_i}$ of an angle ε_i around $\vec{x}_{r_i}$.

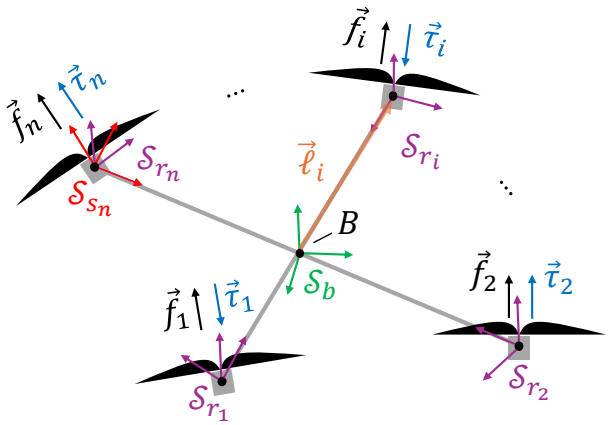

Figure 1. Diagram representing a fully actuated MAV with n rotors.

Each rotor i generates a thrust force $\vec{f}_i \triangleq f_i\vec{z}_{s_i}$ and a reaction torque $\vec{\tau}_i = (-1)^{i+1}\tau_i\vec{z}_{s_i}$, with the magnitudes respectively, given by $f_i \triangleq k_{f_i}\varpi_i^2$ and $\tau_i \triangleq k_{\tau_i}\varpi_i^2$, where $k_{f_i} \in \mathbb{R}_+$ and $k_{\tau_i} \in \mathbb{R}_+$ represent known aerodynamic coefficients and $\varpi_i \in \mathbb{R}_+$ describes the i-th rotor's angular speed.

Consider a constant matrix $\mathbf{D}^{r_i/b}$ that represents the attitude of $\mathcal{S}_{r_i}$ w.r.t. $\mathcal{S}_b$ and an elementary rotation matrix

$$\mathbf{D}^{s_i/r_i}(\varepsilon_i) = \begin{bmatrix} 1 & 0 & 0 \\ 0 & \cos(\varepsilon_i) & \sin(\varepsilon_i) \\ 0 & -\sin(\varepsilon_i) & \cos(\varepsilon_i) \end{bmatrix}$$

representing the attitude of the i-th rotor, displaced by an angle ε_i around axis $\vec{x}_{s_i} = \vec{x}_{r_i}$, w.r.t. $\mathcal{S}_{r_i}$. The control force $\mathbf{f}_b^c \in \mathbb{R}^3$ and the control torque $\boldsymbol{\tau}_b^c \in \mathbb{R}^3$can be represented in $\mathcal{S}_b$ by:

$$\mathbf{f}_b^c = \sum_{i=1}^{n} f_i \left(\mathbf{D}^{r_i/b}\right)^{\mathrm{T}} \left(\mathbf{D}^{s_i/r_i}(\varepsilon_i)\right)^{\mathrm{T}} \mathbf{e}_3 \tag{1}$$

$$\boldsymbol{\tau}_b^c = \sum_{i=1}^{n} \left(\left(f_i \left[\boldsymbol{\ell}_{i,b}\times\right] + (-1)^{i+1}\tau_i\right) \left(\mathbf{D}^{r_i/b}\right)^{\mathrm{T}} \left(\mathbf{D}^{s_i/r_i}(\varepsilon_i)\right)^{\mathrm{T}} \mathbf{e}_3 \right) \tag{2}$$

where $\boldsymbol{\ell}_{i,b} \in \mathbb{R}^3$ is the arm vector, from B towards the S_i, in $\mathcal{S}_b$.

Regarding the modeling of the rotors' spinning dynamics, we consider the following first-order linear time-invariant ODE

$$\dot{\varpi}_i = {T_r}^{-1} \left(-\varpi_i + \overline{\varpi}_i\right), \tag{3}$$

where $T_r \in \mathbb{R}_+$ is a time constant associated with the rotor's physical properties and $\overline{\varpi}_i$ is the i-th rotor's angular speed command. Additionally, assume that ϖ_i is bounded by known variables $\varpi_i^{\min}$ and $\varpi_i^{\max}$:

$$0 \leq \varpi_i^{\min} \leq \varpi_i \leq \varpi_i^{\max}. \tag{4}$$

On the other hand, the thrust vectoring dynamics can be represented by the following second-order model

$$\ddot{\varepsilon}_i = -\omega_{n,i}^2 \varepsilon_i - 2\zeta_i \omega_{n,i} \dot{\varepsilon}_i + \kappa_i \omega_{n,i}^2 \bar{\varepsilon}_i, \tag{5}$$

where $\bar{\varepsilon}_i$ is the vector angle command, $\omega_{n,i}^2$ is the rotor natural frequency, κ_i is a constant coefficient, ζ_i is the damping coefficient (assume $\zeta_i \geq 1$, *i.e.*, the dynamics are over or critically damped) and the vectoring angle is symmetrically bounded by physical limit $\varepsilon_i^{\max}$, which is known and, for practical reasons, assumed to be between 0 and $\pi/2$, *i.e.*, $0 \leq \varepsilon_i^{\max} \leq \pi/2$ and

$$-\varepsilon_i^{\max} \leq \varepsilon_i \leq \varepsilon_i^{\max}. \tag{6}$$

2.3 Control allocation

The force $\bar{\mathbf{f}}_b^c$ and torque $\overline{\boldsymbol{\tau}}_b^c$ commands, which are calculated by the MAV's flight control laws, are related to the $\overline{\varpi}_i$ angular speed commands and $\bar{\varepsilon}_i$ vectoring angle commands through the *control allocation equation*, derived from eqs. (1) and (2):

$$\mathbf{u} = \boldsymbol{\Gamma}\bar{\mathbf{f}} \tag{7}$$

where $\bar{\mathbf{f}} \triangleq \left(\bar{\mathbf{f}}_1, \bar{\mathbf{f}}_2, ..., \bar{\mathbf{f}}_n\right) \in \mathbb{R}^{3n}$, $\bar{\mathbf{f}}_i \triangleq \bar{f}_i \left(0, -\sin\left(\bar{\varepsilon}_i\right), \cos\left(\bar{\varepsilon}_i\right)\right)$, $\bar{f}_i \triangleq k_{f_i} \overline{\varpi}_i^2$, $\mathbf{u} \triangleq \left(\bar{\mathbf{f}}_b^c, \overline{\boldsymbol{\tau}}_b^c\right) \in \mathbb{R}^6$,

$$\boldsymbol{\Gamma} \triangleq \begin{bmatrix} \boldsymbol{\Upsilon}_1 & \boldsymbol{\Upsilon}_2 & \cdots & \boldsymbol{\Upsilon}_n \\ \boldsymbol{\Theta}_1 & \boldsymbol{\Theta}_2 & \cdots & \boldsymbol{\Theta}_n \end{bmatrix} \quad \in \mathbb{R}^{6\times 3n}, \tag{8}$$

with $k_i = k_{\tau_i}/k_{f_i} \in \mathbb{R}_+$, $\boldsymbol{\Theta}_i \triangleq \left(\left[\boldsymbol{\ell}_{i,b}\times\right] + (-1)^{i+1} k_i \mathbf{I}_3\right)\boldsymbol{\Upsilon}_i \in \mathbb{R}^3$ and $\boldsymbol{\Upsilon}_i \triangleq \left(\mathbf{D}^{r_i/b}\right)^{\mathrm{T}}$. Note that $\bar{\mathbf{f}}_i = \left(\mathbf{D}^{s_i/r_i}(\bar{\varepsilon}_i)\right)^{\mathrm{T}} \mathbf{e}_3$.

Since this paper is focused on fully actuated MAVs, assume that $\boldsymbol{\Upsilon}_1, \cdots, \boldsymbol{\Upsilon}_n$ and, consequently, each $\mathbf{D}^{r_i/b}$ are constant matrices such that $\boldsymbol{\Gamma}$ has full rank $\left(\mathrm{rank}\left(\boldsymbol{\Gamma}\right) = 6\right)$, *i.e.*, the positioning of the rotors provide full translational and rotational actuation to the vehicle. The work developed in this paper can be extended to an under-actuated vehicle, without loss of generality, by condensing the corresponding $\boldsymbol{\Gamma}$ matrix to an analogous full-rank matrix and adjusting the dimension of $\bar{\mathbf{f}}_i$.

Hence, the following control allocation problem can be stated.

Problem 1: Control Allocation Problem. The problem of allocating the control efforts $\bar{\mathbf{f}}_b^c$ and $\overline{\boldsymbol{\tau}}_b^c$ consists on finding a set of angular speed commands $\overline{\varpi}_i$ and vectoring angle commands $\bar{\varepsilon}_i$ that satisfy eqs. (4), (6) and (7) for a given $\mathbf{u} \in \mathbb{R}^6$.

3 Problem solving

In this section, the control allocation problem is formulated as a convex optimization one. A method to obtain the rotors' speed and vectoring angle commands from the solution of problem is also provided.

3.1 Control allocation optimization

The goal here is to write Problem 1 in the format of a convex optimization problem. This means that the rotor bounds (eqs. (4) and (6)) must be translated into a convex set. First, let them be written in terms of $\overline{\varpi}_i$ and $\bar{\varepsilon}_i$.

Lemma 1. Consider a rotor with angular speed dynamics described by eq. (3), starting from an initial condition $\varpi_{i,0} \triangleq \varpi_i(t_0)$ where eq. (4) is satisfied. If the command $\overline{\varpi}_i$ is bounded by $\varpi_i^{\min} \leq \overline{\varpi}_i \leq \varpi_i^{\max}$, then the constraints in eq. (4) are satisfied for every $t_1 \geq t_0$.

Proof. The behavior of a first-order systems such as eq. (3) is well known (Ogata [10], Franklin et al. [11]). For a $\Delta t \triangleq t_1 - t_0$, the responses of this system to a constant external input $\overline{\varpi}_i(t_0) = \overline{\varpi}_i(t_0 + \Delta t) = \overline{\varpi}_i$ is given by

$$\varpi_i(t_0 + \Delta t) = \varpi_{i,0} e^{-\Delta t/T_r} + (1 - e^{-\Delta t/T_r})\overline{\varpi}_i. \tag{9}$$

Assume that $\varpi_{i,0} \in \left[\varpi_i^{\min}, \varpi_i^{\max}\right]$ and $\overline{\varpi}_i \in \left[\varpi_i^{\min}, \varpi_i^{\max}\right]$ and note that $e^{-\Delta t/T_r} \in [0,1]$ and $\left(1 - e^{-\Delta t/T_r}\right) \in [0,1]$. Therefore

$$\varpi_i^{\min} e^{-\Delta t/T_r} + \varpi_i^{\min}(1 - e^{-\Delta t/T_r}) \leq \varpi_i(t_0 + \Delta t) \leq \varpi_i^{\max} e^{-\Delta t/T_r} + \varpi_i^{\max}(1 - e^{-\Delta t/T_r}) \tag{10}$$

$$\therefore \varpi_i^{\min} \leq \varpi_i(t_1) \leq \varpi_i^{\max}. \tag{11}$$

Lemma 2. Consider a rotor with vectoring angle dynamics described by eq. (5), starting from an initial condition $(\varepsilon_{i,0}, \dot{\varepsilon}_{i,0}) \triangleq (\varepsilon_i(t_0), \dot{\varepsilon}_i(t_0))$ where eq. (6) is satisfied. If $\dot{\varepsilon}_{i,0} = 0$ and the command $\bar{\varepsilon}$ is bounded by $-\varepsilon_i^{\max} \leq \bar{\varepsilon}_i \leq \varepsilon_i^{\max}$, then the constraints in eq. (6) are satisfied for every $t_1 \geq t_0$.

Proof. The response of the system described by eq. (5) to a constant external input when $\zeta_i = 1$, *i.e.* when the system is critically damped, is given by

$$\varepsilon_i(t_0 + \Delta t) = \varepsilon_{i,0}(1 + \omega_{n,i}\Delta t)e^{-\omega_{n,i}\Delta t} + \dot{\varepsilon}_{i,0}\Delta t e^{-\omega_{n,i}\Delta t} + \left(1 - (1 + \omega_{n,i}\Delta t)e^{-\omega_{n,i}\Delta t}\right)\kappa_i\bar{\varepsilon}_i \tag{12}$$

If $\dot{\varepsilon}_{i,0}$ is negligible, which means that the command only changes after the the system has reached or is very close to the previous commanded position, then we get a response very similar to eq. (9):

$$\varepsilon_i(t_0 + \Delta t) = \varepsilon_{i,0}(1 + \omega_{n,i}\Delta t)e^{-\omega_{n,i}\Delta t} + \left(1 - (1 + \omega_{n,i}\Delta t)e^{-\omega_{n,i}\Delta t}\right)\kappa_i\bar{\varepsilon}_i \tag{13}$$

Assume that $\varepsilon_{i,0} \in [-\varepsilon_i^{\max}, \varepsilon_i^{\max}]$, $\bar{\varepsilon}_i \in [-\varepsilon_i^{\max}, \varepsilon_i^{\max}]$ and $\omega_{n,i} \geq 0$ and note that $(1 + \omega_{n,i}\Delta t)e^{-\omega_{n,i}\Delta t} \in [0,1]$ and $\left(1 - (1 + \omega_{n,i}\Delta t)e^{-\omega_{n,i}\Delta t}\right) \in [0,1]$. Following the same steps as the proof for Lemma 1, we obtain:

$$-\varepsilon_i^{\max} \leq \varepsilon_i(t_1) \leq \varepsilon_i^{\max}. \tag{14}$$

The proof for $\zeta_i > 1$ is analogous.

Now, using eq. (11) and the definitions of $\bar{f}_i$ and $\bar{\mathbf{f}}_i$ in section 2.3, we arrive to:

$$k_f(\varpi_i^{\min})^2 \leq \bar{f}_i \leq k_f(\varpi_i^{\max})^2 \tag{15}$$

and $\tan(\bar{\varepsilon}_i) = -\dfrac{\mathbf{e}_2^{\mathrm{T}}\bar{\mathbf{f}}_i}{\mathbf{e}_3^{\mathrm{T}}\bar{\mathbf{f}}_i}$. For the interval in eq. (6), the tangent function is strictly increasing, hence:

$$\mathbf{\Lambda_1}\bar{\mathbf{f}}_i \leq \mathbf{0}, \tag{16}$$

where:

$$\mathbf{\Lambda}_1 \triangleq \begin{bmatrix} \mathbf{e}_2^{\mathrm{T}} + \tan(\varepsilon_i^{\min})\mathbf{e}_3^{\mathrm{T}} \\ -\mathbf{e}_2^{\mathrm{T}} - \tan(\varepsilon_i^{\max})\mathbf{e}_3^{\mathrm{T}} \end{bmatrix} \tag{17}$$

The set of forces that comply with the constraints in eqs. (15) and (16) is not convex, except when $\varpi_i^{\min} = 0$. A convex subset $\mathcal{C}_i$, however, can be obtained by limiting the force components $\bar{f}_{ri,z}$ to an inferior limit $\bar{f}_{ri,z}^{\min} \triangleq k_f(\varpi_i^{\min})^2$. With this subset, a convex optimization problem with linear constraints whose solution conservatively solves the control allocation problem can be defined.

Problem 2: Convex Optimization. Given $\mathbf{u} \in \mathbb{R}^6$ and a differentiable convex cost function $J : \mathbb{R}^6 \to \mathbb{R}$, find a control allocation $\bar{\mathbf{f}}^*$ that solves the convex optimization problem

$$\bar{\mathbf{f}}^* = \quad \operatorname{argmin} J(\bar{\mathbf{f}}) \tag{18}$$

$$\text{subject to } \mathbf{u} = \mathbf{\Gamma}\bar{\mathbf{f}} \tag{19}$$

$$\bar{\mathbf{f}} \in \mathcal{C} \tag{20}$$

where $\mathcal{C} \triangleq \mathcal{C}_1 \times ... \times \mathcal{C}_n$, with $\mathcal{C}_i \triangleq \left\{\bar{\mathbf{f}}_i \in \mathbb{R}^3 : \bar{f}_i \leq k_f(\varpi_i^{\max})^2, \mathbf{\Lambda_2}\bar{\mathbf{f}}_i \leq \left(0, 0, -\bar{f}_{zri}^{\min}\right)\right\}$ and $\times$ representing the Cartesian product, where

$$\mathbf{\Lambda_2} = \begin{bmatrix} \mathbf{e}_2^{\mathrm{T}} + \tan(\varepsilon_i^{\min})\mathbf{e}_3^{\mathrm{T}} \\ -\mathbf{e}_2^{\mathrm{T}} - \tan(\varepsilon_i^{\max})\mathbf{e}_3^{\mathrm{T}} \\ -\mathbf{e}_3^{\mathrm{T}} \end{bmatrix}. \tag{21}$$

Well known optimization methods, such as the interior point method proposed by Boyd and Vandenberghe [12], are used to solve Problem 2 numerically and obtain an optimal $\bar{\mathbf{f}}_i$. The optimal commands for the effectors can be obtained inverting the thrust force equations:

$$\overline{\varpi}_i^* = \sqrt{\frac{||\bar{\mathbf{f}}_i^*||}{k_f}} \tag{22}$$

$$\bar{\varepsilon}_i^* = \arctan\left(-\frac{\mathbf{e}_2^T\bar{\mathbf{f}}_i^*}{\mathbf{e}_3^T\bar{\mathbf{f}}_i^*}\right) \tag{23}$$

4 Simulation example

A fully actuated hexacopter was modeled in order to exemplify and analyze through simulation the proposed control allocation method. This model represents a vehicle with mass m = 0.5kg, inertia matrix $\mathbf{J}_b = 0.01\mathbf{I}_3$ kgm^2 and rotor arms ℓ = 0.25 m and the six rotors were considered identical using this modeling parameters: $k_f = 2.5 \times 10^{-5}$ kgm/rad^2, $k_t = 5.0 \times 10^{-7}$ kgm^2/rad^2, $\varpi^{\max}$ = 500 rad/s, $\varpi^{\min}$ = 100 rad/s, $T_m = 0.01$, $\varepsilon^{\max}$ = $\pi/3$ rad, $\varepsilon^{\min} = -\varepsilon^{\max} = -\pi/3$ rad, $\omega_n = 500$ rad/s and $\zeta = 0.8$.

4.1 Static Analysis

The proposed method was applied to 1000 random effort commands $\mathbf{u}$ and the errors and bound violations were quantified. The results were compared with a relaxed optimal control allocator (Dyer et al. [13]) and with a pseudo-inverse allocator similar to the ones proposed by Rajappa et al. [14], Santos and Cunha [15].

Table 1. Static comparison between different control allocation methods.

Control allocation method	*Proposed*	*Pseudo-inverse*	*Relaxed*
Violations	0	1214	0
Force error (normalized)	0	8.8574	1.3345
Torque error (normalized)	0	11.0873	0.9997
Max. time (s)	0.1139	0.0063	0.1523
Mean time (s)	0.0420	0.0009	0.0438

4.2 Dynamic Analysis

For an analysis of the dynamic effects of the proposed control allocation method, the simulated hexacopter was commanded to reach both a position reference $\mathbf{r} = (10, 10, 10)$ m and an attitude reference $\boldsymbol{\sigma} = (-30, 30, 30)$

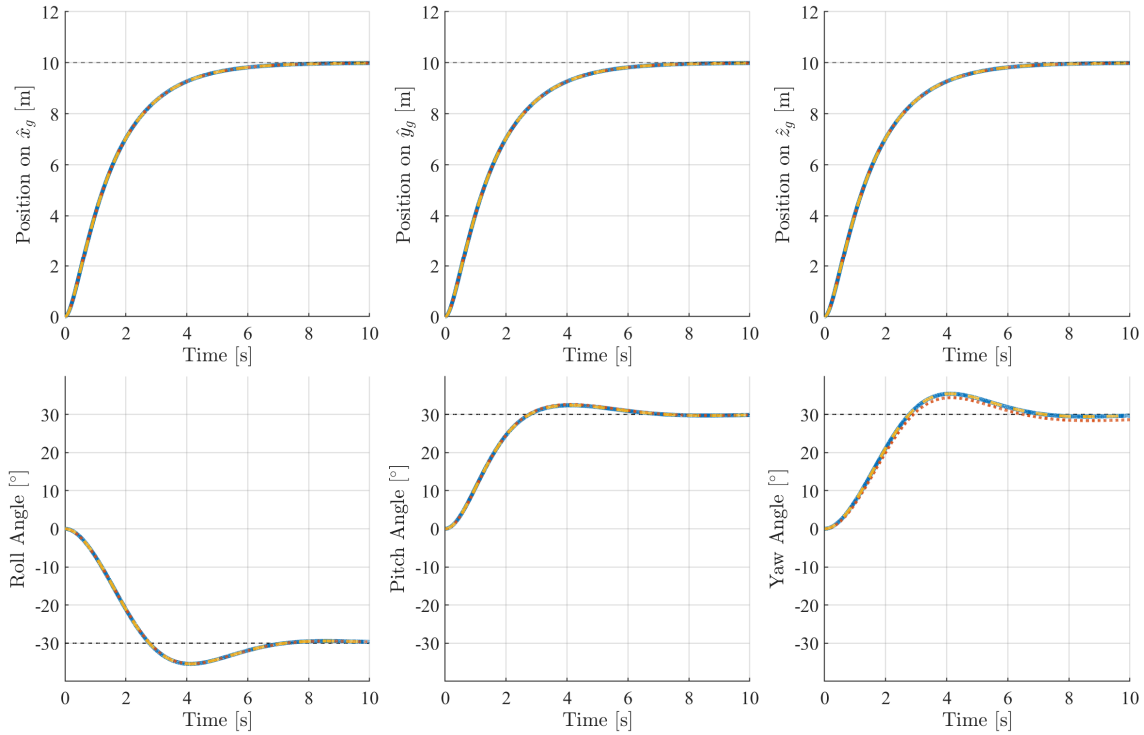

Figure 2. Hexacopter's translational and rotational displacements. The dashed black line represents the reference input to the control system and the lines in blue, red, and yellow, represent the dynamic response for the proposed, relaxed, and pseudo-inverse control allocation methods, respectively.

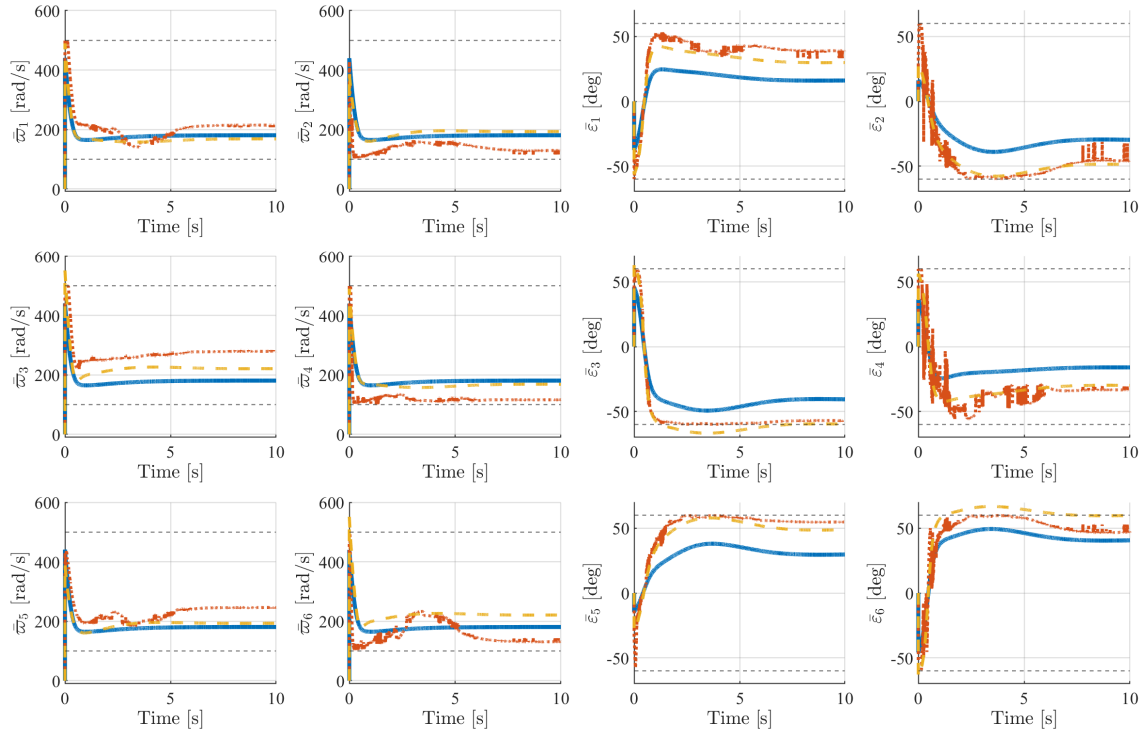

Figure 3. Angular speed and vectoring angle commands for the six rotors. The dashed black line represents the rotor's bounds and the lines in blue, red, and yellow, represent the commands generated by the proposed, relaxed, and pseudo-inverse control allocation methods, respectively.

deg. As shown by Fig. 2, all the 3 methods reach the commanded references within the simulation time ($t = 10$ s) and following the same path.

From Fig. 3, we immediately observe that the pseudo-inverse method does not respect the effectors' bounds. Comparing the both optimization methods (relaxed and proposed), is easy to see that the commands generated by the proposed method are smoother and, in general, farther from the actuation limits.

5 Conclusions

The control allocation method proposed in this paper meets the performance provided by similar methods available in the literature while ensuring that the limits of both the rotors and vectoring actuators are respected, as shown in section 4. The definition of a systematic approach to handle the inherit non-convexity of the rotors' minimum thrust bounds, made the method applicable to a even broader set of MAV configurations.

Acknowledgements. The authors would like to thank FINEP for the financial support under grant 01.22.0069.00. The first author is grateful to ITA's Graduate Program on Aeronautics and Mechanics Engineering. The second author is grateful for the support of the CNPq, under grant 304300/2021-7.

Authorship statement. The authors hereby confirm that they are the sole liable persons responsible for the authorship of this work, and that all material that has been herein included as part of the present paper is either the property (and authorship) of the authors, or has the permission of the owners to be included here.

References

[1] P. Höhrová, J. Soviar, and W. Sroka. Market analysis of drones for civil use. *LOGI – Scientific Journal on Transport and Logistics*, vol. 14, n. 1, pp. 55–65, 2023.

[2] H. Shakhatreh, A. H. Sawalmeh, A. Al-Fuqaha, Z. Dou, E. Almaita, I. Khalil, N. S. Othman, A. Khreishah, and M. Guizani. Unmanned aerial vehicles (uavs): A survey on civil applications and key research challenges. *IEEE Access*, vol. 7, pp. 48572 – 48634. Cited by: 1263; All Open Access, Gold Open Access, Green Open Access, 2019.

[3] R. Kumar, A. Nemati, M. Kumar, R. Sharma, K. Cohen, and F. Cazaurang. Tilting-Rotor Quadcopter for Aggressive Flight Maneuvers Using Differential Flatness Based Flight Controller. volume 3 of *Dynamic Systems and Control Conference*, pp. V003T39A006, 2017.

[4] M. Saied, H. Shraim, and C. Francis. A review on recent development of multirotor uav fault-tolerant control systems. *IEEE Aerospace and Electronic Systems Magazine*, vol. , pp. 1–30, 2023.

[5] J. A. Bezerra and D. A. Santos. Optimal exact control allocation for under-actuated multirotor aerial vehicles. *IEEE Control Systems Letters*, vol. 6, pp. 1448–1453, 2022a.

[6] J. A. Bezerra and D. A. Santos. On the guidance of fully-actuated multirotor aerial vehicles under control allocation constraints using the receding-horizon strategy. *ISA Transactions*, vol. 126, pp. 21–35, 2022b.

[7] A. L. Silva and D. A. Santos. Fast nonsingular terminal sliding mode flight control for multirotor aerial vehicles. *IEEE Transactions on Aerospace and Electronic Systems*, vol. 56, n. 6, pp. 4288 – 4299, 2020.

[8] M. Kirchengast, M. Steinberger, and M. Horn. Control allocation under actuator saturation: An experimental evaluation. *IFAC-PapersOnLine*, vol. 51, n. 25, pp. 48–54. 9th IFAC Symposium on Robust Control Design ROCOND 2018, 2018.

[9] S. Park, J. Her, J. Kim, and D. Lee. Design, modeling and control of omni-directional aerial robot. In *2016 IEEE/RSJ International Conference on Intelligent Robots and Systems (IROS)*, pp. 1570–1575, 2016.

[10] K. Ogata. *Modern Control Engineering*. Pearson Prentice Hall, 5th edition, 2010.

[11] G. Franklin, J. Powell, and A. Emami-Naeini. *Feedback Control of Dynamic Systems*. Addison-Wesley series in electrical and computer engineering: Control engineering. Addison-Wesley, 1994.

[12] S. Boyd and L. Vandenberghe. *Convex Optimization*. Cambridge University Press, 2004.

[13] E. Dyer, S. Sirouspour, and M. Jafarinasab. Energy optimal control allocation in a redundantly actuated omnidirectional uav. In *2019 International Conference on Robotics and Automation (ICRA)*, pp. 5316–5322, 2019.

[14] S. Rajappa, M. Ryll, H. H. Bülthoff, and A. Franchi. Modeling, control and design optimization for a fully-actuated hexarotor aerial vehicle with tilted propellers. In *2015 IEEE International Conference on Robotics and Automation (ICRA)*, pp. 4006–4013, 2015.

[15] D. A. Santos and A. Cunha. Flight control of a hexa-rotor airship: Uncertainty quantification for a range of temperature and pressure conditions. *ISA Transactions*, vol. 93, pp. 268–279, 2019.